Ab initio interpolated potential energy surface and classical reaction dynamics for H C O + + H , H O C + + H , and deuterated analogues

Gloria E. Moyano, Seth A. Jones, and Michael A. Collins

Citation: The Journal of Chemical Physics **124**, 124318 (2006); doi: 10.1063/1.2181571
View online: http://dx.doi.org/10.1063/1.2181571
View Table of Contents: http://scitation.aip.org/content/aip/journal/jcp/124/12?ver=pdfcov
Published by the AIP Publishing

Ab initio interpolated potential energy surface and classical reaction dynamics for $HCO^+ + H$, $HOC^+ + H$, and deuterated analogues

Gloria E. Moyano, Seth A. Jones, and Michael A. Collins[a)]
Research School of Chemistry, Australian National University, Canberra, Australian Capital Territory 0200, Australia

(Received 13 December 2005; accepted 7 February 2006; published online 28 March 2006)

Classical simulations of the reactions between HCO^+/COH^+ and hydrogen atoms, as well as their deuterated variants, have been carried out on an *ab initio* interpolated potential energy surface. The surface is constructed at the quadratic configuration interaction with single and double excitation level of *ab initio* calculation. At low energies we observe reaction channels associated with the isomerization of the cation, hydrogen/deuterium exchange, and the combination of isomerization with exchange. The HCO^+/DCO^+ ions only undergo exchange, and deuteration is more facile than the release of deuterium. The COH^+/COD^+ ions undergo isomerization or isomerization combined with exchange, the latter being the dominant reaction channel. Deuteration is again more facile than the release of deuterium, in combination with isomerization. These results are consistent with experimental measurements and with hypotheses on the deuteration of molecules in the interstellar medium. © *2006 American Institute of Physics*. [DOI: 10.1063/1.2181571]

I. INTRODUCTION

According to the current models of interstellar chemistry, the formyl ion HCO^+ and its isomer HOC^+ occur in the interstellar medium (ISM) as products of the reaction of $H_3^+ + CO \rightarrow (HCO^+ \text{ or } HOC^+) + H_2$. In photon dominated regions of the ISM, the isoformyl ion can also be obtained as the main product of the reaction $C^+ + H_2O \rightarrow HOC^+ + H$.[1,2] HCO^+ is the most stable of the two isomers, and its abundance is several orders of magnitude higher than that of HOC^+ as determined in several sources.[2,3]

The HCO^+ and HOC^+ ions participate in a complex network of chemical reactions which give rise to larger polyatomic molecules in the ISM. This chemistry also involves the isotope exchange promoted by reactions such as

$$D + HCO^+ \rightarrow DCO^+ + H, \tag{1.1}$$

which plays a key role in the fractionation of deuterium in the ISM.[4,5]

In the gas phase, HOC^+ can isomerize to HCO^+ only over a classical potential energy barrier of 155.6 kJ/mol [146.0 kJ/mol with zero point vibrational energy (ZPVE) correction], according to a very accurate coupled cluster calculation.[6] This barrier prevents the isomerization in conditions similar to those of the ISM. It has been established by *ab initio* studies that the interaction of isoformyl ion with various neutral species X, according to the scheme

$$X + HOC^+ \rightarrow [XH \ldots OC]^+ \rightarrow [OC \ldots XH]^+ \rightarrow OCH^+ + X, \tag{1.2}$$

can lower the barrier height and therefore catalyze the isomerization.[7–9] This catalytic action has been referred to as proton-transport, ion-transport, or a chaperone mechanism (see, e.g., Refs. 3, 7, and 8 and references cited therein). According to the energy of the reaction profiles, the extent to which the barrier is lowered depends upon the nature of the species X. Whenever the proton affinity of the species X lies between the proton affinities of CO at O and C, respectively, there is an effective catalysis as the barrier becomes negative (e.g., $X = HF, N_2$). If the proton affinity of X is below that range, the barrier is reduced but remains positive (e.g., $X = He, Ne, Ar$). Species with proton affinities higher than those of CO (e.g., $X = H_2O, NH_3$) produce the largest reductions of the barrier, but then the intermolecular proton transfer

$$X + HOC^+ \rightarrow XH^+ + CO \tag{1.3}$$

becomes energetically preferred to the intramolecular proton transport of (1.2).[7]

Classical dynamics investigations of collisions between HOC^+ and a rare gas atom have shown that the rare gas atoms either do not catalyze the isomerization (1.2) at low temperature ($X = Ne, Ar$) or have some catalytic effect, but the isomerization competes with the abstraction (1.3) ($X = Kr$).[8] This occurs despite the barriers to isomerization being lower than those of the abstraction,[7,8] and the competition favors the abstraction as soon as the collision energies allow this reaction.[8]

The situation becomes more complex for collisions of HOC^+ with HF and H_2O. In these cases besides proton transfer and proton abstraction there are the possibilities of proton exchange,

$$H'Y + HOC^+ \rightarrow HY + H'OC^+, \tag{1.4}$$

and the combined proton exchange rearrangement,

[a)]Electronic mail: collins@rsc.anu.edu.au

$$H'Y + HOC^+ \rightarrow HY + H'CO^+. \quad (1.5)$$

The abstraction reaction was found to be the dominant channel in classical collision studies of both systems, for reactants in their lowest vibrational levels.[9] It was suggested that the abstraction is preferred because it does not involve complicated molecular rearrangements in the ion-molecule complex. Such a complex was not always formed during the collisions.[9] There are some detailed studies in the literature of the energy profiles for the reactions between the isoformyl ion and hydrogen atoms.[3,10] However, there are no classical or quantum reaction dynamics treatments of the reactions.

In this paper we present an accurate, ground state, molecular potential energy surface (PES) for the dynamics of the collisions between formyl/isoformyl ions with hydrogen atoms and analogous deuterated reactions. The PES has been constructed iteratively by an interpolation method on a sparse set of *ab initio* data points. The *ab initio* energies and energy derivatives at each data point were calculated using the quadratic configuration interaction including single and double substitutions (QCISD) approximation. Results from the classical dynamics for these collisions at low energies are also reported. These are analyzed in comparison with the corresponding dynamics previously observed for closed shell systems.[8,9] The dynamics for conditions similar to those of the ISM are also discussed in terms of the calculated minimum energy path reaction profiles.[3] The PES reported here provides a basis for future quantum dynamics calculations of the cross sections for the hydrogen/deuterium exchange and the isomerization reactions.

The paper is set out as follows. Section II presents a brief description of the method for the interpolation of the PES and the modifications implemented to treat this reactive system. This section also contains basic considerations on the quantum chemistry of the system, such as the stationary structures involved, reaction paths, and *ab initio* approximations suitable for the construction of the PES. The computational details of the classical dynamics calculations are also in Sec. II. Section III describes the characteristics and accuracy of the PES, the dynamics results, and the discussion. Section IV presents some concluding remarks.

II. METHODOLOGY

A. Construction of the interpolated PES

The PES in this work is computed by an interpolation method whose details have been presented previously.[11–14] According to this method, the potential energy at some molecular configuration $\mathbf{Z}$ is given by the expression

$$E(\mathbf{Z}) = \sum_{g \in G} \sum_{i=1}^{N_{\text{data}}} w_{g \circ i}(\mathbf{Z}) T_{g \circ i}(\mathbf{Z}), \quad (2.1)$$

which combines a number N_{data} of local Taylor expansions T_i of the energy, around a sparse set of molecular configurations $\mathbf{Z}(i)$, as a weighted average. The N_{data} molecular configurations associated with the Taylor expansions are known as the "data set," and each element of the data set is called a "data point." The Taylor expansions are calculated from *ab initio* energies, gradients, and Hessians at each of the data points. The independent coordinates used in the expansions are $3N-6$ linear combinations of the inverse interatomic distances, $\mathbf{Z}=\{Z_1, \ldots, Z_k, \ldots, Z_{N(N-1)/2}\}$, where $Z_k = 1/R_k$.

The weights w_i in (2.1) are dependent upon the distance coordinates $\mathbf{Z}$ with respect to a data point configuration $\mathbf{Z}(i)$. They also include a "confidence volume" around each data point.[11,12] The confidence volumes for the PES in this work were evaluated using an energy tolerance, $E_{\text{tol}} = 0.525$ kJ mol^{-1}, and energy gradients at $M = 100$ data points (see Ref. 11 for definitions of E_{tol} and M).

The permutational symmetry of indistinguishable nuclei is taken into account in (2.1) through the sum over $g \in G$, where g is an element of the complete nuclear permutation (CNP) group G of the molecular system. If $\mathbf{Z}(i)$ is a data point, then the permuted configuration $g \circ \mathbf{Z}(i)$ (abbreviated to $g \circ i$) is also a data point. This way, the Taylor expansions at a data point, and all data points related by permutations, are constructed from a single set of *ab initio* quantities, and the PES has the required permutational invariance.

The data set for an interpolated PES is obtained by iterative addition of molecular configurations to an initial set of configurations characteristic of the PES. The initial set usually contains the stationary points associated with all reaction paths relevant for the conditions, as well as other points sampled along those paths. Further data points are sampled one by one from classical trajectory simulations of the reaction dynamics performed on the interpolated PES over the current data set at each iteration. The sampling of trajectory points is done according to criteria known as the "variance sampling"[14] and the "h-weight sampling."[12,13,15]

The addition of data points is continued until the PES is deemed to be converged. The convergence in this method is evaluated by monitoring the interpolation error and the values of dynamic quantities such as reaction cross sections at different stages during the construction of the PES. When those quantities do not change beyond some tolerance with the increase of the number of data points, the PES is considered converged. Only at this stage is the PES reliable for sufficiently accurate classical trajectory or quantum simulations of the reaction dynamics.

The systematic procedure summarized here has been implemented as algorithms in the program suite GROW.[12]

B. Quantum chemistry methods

Some previous *ab initio* studies of the ground state molecular PES for the system $[H_2CO]^{\cdot+}$ have been performed at the restricted and unrestricted Hartree-Fock (HF) and Moller-Plesset perturbation (MP2) levels of approximation (see Refs. 3 and 10 and references cited therein). This work provided information about relevant stationary points and minimum energy paths (MEP). The data were reevaluated here by more accurate treatments for three purposes: first, to establish what molecular species are involved in the possible reactions, second, to provide an initial set of configurations for our interpolated PES, and third, to select *ab initio* approximations which provide a sufficiently accurate PES. The *ab initio* calculations for this paper were performed using the

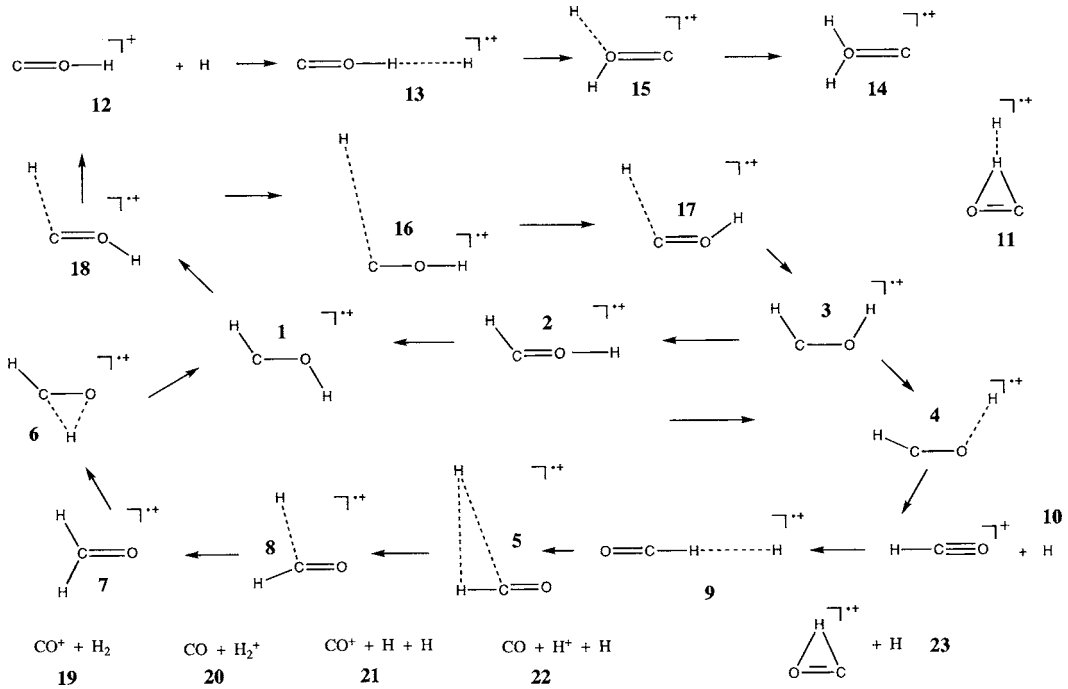

FIG. 1. The geometries of the stationary points on the H_2CO^+ PES are shown schematically. The arrows are intended to indicate the relative location of some geometries on minimum energy reaction paths.

GAUSSIAN 98 (Ref. 16) and GAUSSIAN 03 (Ref. 17) suites of programs.

Figure 1 shows a pictorial representation of the stationary points identified and characterized on the PES of $[H_2CO]^{\cdot+}$ at the QCISD/6-311G(d,p) level of *ab initio* calculation. The corresponding geometrical parameters are shown in Table I. Evaluation of these parameters using the Hartree-Fock method gave similar values, except that structure 2 is nonplanar at the HF level, with a HCOH dihedral angle of 90.3°. Moreover, some configurations, 1, 3, 5, 7, 9, 10, 12, 13, 14, and 16 in Fig. 1, had been characterized as local minima on the PES by vibrational analysis performed

TABLE I. The geometrical parameters of stationary points on the H_2CO^+ PES are shown, as determined at the QCISD/6-311G(d,p) level of theory. The structure numbers refer to Fig. 1. Bond lengths are shown in angstroms and angles in degrees.

Structure	R(CO)	R(CH_a)	R(CH_b)	R(OH_a)	R(OH_b)	R(HH)	∠OCH_a	∠OCH_b	∠COH_b
1	1.225	1.101			0.986		124.4		116.7
2	1.202	1.109			0.976		125.8		180.0
3	1.220	1.102			0.989		131.6		119.1
4	1.145	1.095			1.502		158.4		123.4
5	1.111	1.094	2.997			2.917	179.4		105.4
6	1.220	1.106			1.234		134.7		64.3
7	1.202	1.116	1.116				119.3		
8	1.122	1.095	1.867				162.1	106.7	
9	1.111	1.105				1.900	180	180	
10	1.110	1.095					180		
11	1.155	1.634	2.454			0.962	63.2		
12	1.162				0.992				180
13	1.160				1.037	1.416			
14	1.407			0.984	0.984				121.9
15	1.228	1.997		0.991	1.459				127.3
16	1.163	3.249			0.991		100.3		179.1
17	1.172	2.250			0.990		111.3		154.6
18	1.172	2.234			0.990		108.0		152.8
19	1.120					0.744			
20	1.134					1.049			
21	1.120								
22	1.134								
23	1.154				1.368				61.2

TABLE II. The energies (kJ mol^{-1}), relative to the separated reactants COH^++H (structure 12 in Fig. 1), of stationary geometries optimized with the methods shown using a 6-311G(d,p) basis set.

Structure	HF	B3LYP	QCISD
1	−244.8	−285.0	−253.9
2	−169.1	−219.6	−176.9
3	−231.2	−268.9	−236.8
4	−32.0	−140.3	−84.9
5	−138.2	⋯	−168.4
6	−19.2	−111.8	−76.4
7	−280.3	−314.0	−281.2
8	−113.0	⋯	−154.9
9	−141.3	−180.1	−173.0
10	−137.3	−164.0	−167.0
11	134.4	⋯	78.0
13	−13.6	−40.1	−22.6
14	−43.3	−58.2	−39.6
15	150.8	48.0	106.9
16	−0.3	⋯	−0.5
17	5.6	⋯	2.4
18	6.1	⋯	3.8
19	61.2	38.4	23.2
20	201.0	171.0	194.9
21	409.9	498.4	466.1
22	467.1	452.7	460.9
23	215.4	160.3	161.5

in previous work at the UHF/4-31G (Ref. 3) and HF/(6-31G(d,p) or 6-31G(d)) (Refs. 10 and 18) levels. Configurations 2, 4, 6, 8, 15, 17, and 18 in Fig. 1 had been characterized as first order saddle points (transition states) on the PES by vibrational analysis at the HF/(6-31G(d,p) and 6-31G(d)) levels.[10,18] The critical configurations 11 and 15 were not reported in the previous studies. We obtained them here using guesses based on the structures from Green's paper[3] and characterized them as transition states at various levels.

To indicate the variation of the PES and critical geometries with level of *ab initio* theory, the configurations in Fig. 1 were optimized and characterized by vibrational analysis at the Hartree-Fock, B3LYP, and QCISD levels of approximation [all with a 6-311G(d,p) basis set]. The relative energies of the optimized geometries at the three *ab initio* levels are presented in Table II.

Ideally, dynamical simulations should be carried out on a PES which is as accurate as possible. However, a very large number of *ab initio* calculations are required to characterize a multidimensional PES, so that a compromise between accuracy and computational cost is necessary. In order to determine what level of *ab initio* theory is necessary to describe the molecular PES to sufficient accuracy, calculations of the energy of the QCISD/6-311G(d,p) stationary point geometries were carried out for a wide range of *ab initio* methods and basis sets. Table III presents the results of a selected subset of these calculations. The energies are reported relative to the energy of the $H+COH^+$ reactants, as we consider this to be the most physically relevant reference.

Tables II and III indicate that the HF, B3LYP, and MP2 levels of theory are not adequate. According to Table III the QCISD/cc-pVTZ single point energies reproduce reasonably well the results given by the most reliable CCSD(T)/cc-pV5Z approximation. While the basic topology of the HF and MP2 surfaces agrees with that of the CCSD(T)/cc-pV5Z surface, the energies are inaccurate in some regions. The topology of the B3LYP surface differs from the most reliable surface, as indicated by the fact that some critical points (configurations 5, 8, 11, 16, 17, and 18) in Table II are absent in the B3LYP approximation. Compared to the QCISD/cc-pVTZ surface, the use of larger basis sets, or the use of higher correlation methods, does not yield significant im-

TABLE III. The energies (kJ mol^{-1}) of the QCISD/6-311G(d,p) stationary geometries (see Fig. 1), relative to that of structure 12, are shown for different basis sets and levels of *ab initio* calculation.

	MP2		QCISD				CCSD(T)			
Structure	6-311G(d,p)	cc-pVTZ	6-311G(d,p)	cc-pVTZ	cc-pVQZ	cc-pV5Z	6-311G(d,p)	cc-pVTZ	cc-pVQZ	cc-pV5Z
1	−249.5	−259.7	−253.9	−265.5	−267.2	−268.0	−249.8	−261.4	−263.2	−263.9
2	−174.0	−186.4	−176.9	−190.4	−193.5	−194.6	−172.8	−186.8	−190.1	−191.3
3	−232.3	−244.1	−236.8	−249.9	−251.8	−252.6	−232.5	−245.6	−247.5	−248.3
4	−61.6	−67.5	−84.9	−91.6	−93.4	−94.2	−85.9	−93.5	−95.8	−96.7
5	−198.8	−196.3	−168.4	−167.1	−168.6	−169.1	−170.2	−169.0	−170.7	−171.3
6	−69.2	−82.8	−76.4	−90.1	−90.4	−90.9	−77.8	−92.3	−92.9	−93.6
7	−240.5	−246.2	−281.2	−289.8	−289.1	−289.3	−275.8	−283.9	−283.1	−283.1
8	−167.8	−171.7	−154.9	−159.4	−161.1	−161.7	−156.3	−161.4	−163.5	−164.3
9	−203.0	−201.2	−173.0	−172.5	−173.4	−173.7	−175.0	−174.6	−175.8	−176.1
10	−197.5	−192.7	−167.0	−163.4	−163.7	−163.8	−168.8	−165.2	−165.7	−165.9
11	92.2	85.8	78.0	72.4	71.4	70.8	73.5	66.9	65.4	64.7
13	−24.6	−28.0	−22.6	−26.0	−26.5	−26.7	−23.4	−27.2	−27.8	−28.0
14	−15.3	−19.9	−39.6	−46.0	−45.6	−45.7	−33.4	−39.9	−39.3	−39.3
15	129.1	122.2	106.9	100.7	99.9	99.5	104.9	97.6	96.6	96.1
16	−0.5	−1.7	−0.5	−1.8	−2.5	−2.8	−0.6	−1.8	−2.5	−2.9
17	6.9	2.1	2.4	−3.1	−4.7	−5.2	2.5	−3.2	−4.8	−5.4
18	8.9	4.0	3.8	−1.8	−3.4	−3.9	4.0	−1.8	−3.5	−4.1

provement in the relative energies, considering the additional computational cost. Importantly, the QCISD/cc-pVTZ method yields reasonably accurate energies for structures 4, 5, 16, 17, and 18 which lie towards the reactant and product asymptotes. At low energy, relevant to the ISM, barriers in the entrance channel particularly must have a significant influence on the rate of reaction. It is important to describe such configurations as accurately as possible. Thus, while the QCISD/6-311G(d,p) level of theory is moderately accurate, compared to the CCSD(T)/cc-pV5Z approximation, it yields energies for structures 17 and 18 that lie above the $H+COH^+$ reactants. From such considerations, it appears that the QCISD/cc-pVTZ level is the most computationally efficient approximation, which is sufficiently accurate in the most significant regions of the PES.

The computation of an interpolated PES for four atoms requires the evaluation of the energies, energy gradients, and second derivatives at several hundred molecular configurations. Considering the computational cost, the energy of each data point was evaluated at the QCISD/cc-pVTZ level, while the gradients and Hessians were evaluated at the less costly QCISD/6-311G(d,p) level. In a number of interpolated PESs, the gradients and Hessians have been calculated at a lower level of theory than that used for the energy of each data point. This appears to provide a satisfactory interpolation for the PES when the lower level of theory yields energies which only differ from the higher level values by a few kJ mol^{-1}. However, tests of the general applicability of this approximation would be useful. In a modification of the usual approach to this "mixed level" method in GROW, the QCISD/cc-pVTZ energies at each data point were calculated and used at each iteration of the construction procedure, instead of the QCISD/6-311G(d,p) values.

It is necessary to choose an initial data set for the PES interpolation. The relevant minimum energy paths linking the stationary points were computed at the HF/6-311G(d,p) level from all transition state configurations in order to sample molecular configurations which are relevant to the reactions of interest. Configurations from these paths, configurations towards the $HOC^+/HCO^+ + H$ and $CO^+ + H_2$ asymptotes, and the stationary geometries at the QCISD/6-311G(d,p) level were chosen for the initial data set (containing 244 points) for the interpolated PES.

The interpolated PES can only be accurate for the energy range over which *ab initio* data are incorporated in the data set. This study examines relatively low energy collisions of H atoms with HCO^+ and HOC^+ (and deuterated analogues). The maximum total energy of the system is given by the vibrational energy of the HOC^+ reactant and the relative translational energy. The classical simulations were initiated for reactants with ZPVE. The ZPVEs for the reactant and their deuterated forms are reported in Table IV. The initial translational energy was up to about 13.1 kJ mol^{-1}. Hence, the PES reported here is reliable for energies up to about 48 kJ mol^{-1} above the energy of the $H+HOC^+$ asymptote. *Inter alia*, this implies that high energy regions, including such structures as 11 and 19–23, are not accurately described by the PES reported here.

TABLE IV. The zero point vibrational energies (ZVPE) of the reactants, calculated in the harmonic approximation with a 6-311G(d,p) basis set.

	ZPVE (kJ mol^{-1})	
Species	B3LYP	QCISD
HCO^+	43.2	43.2
DCO^+	36.1	···
COH^+	35.0	35.2
COD^+	28.8	···

C. Classical dynamics

Classical dynamics simulations were performed for the sampling of molecular configurations during the construction of the PES, as well as for the calculation of the reaction cross sections. At each iteration during the construction of the PES, batches of ten trajectories for the collision between either DCO^+ or COD^+ and H were run. The trajectories were calculated with a velocity-Verlet integration algorithm, using a time step size of 1.0×10^{-17} s, starting with a fragment-to-fragment center of mass separation of 10.6 Å and an impact parameter of zero. The reactant molecules were given random orientation, zero rotational angular momentum, and vibrational energies corresponding to their ZPVE level (see Table IV). The relative kinetic energies between the fragments were in a range of 13.1–26.3 kJ mol^{-1}. The initial atomic velocities and configurations for the reactants were generated using the efficient microcanonical sampling method of Schranz *et al.*[19] A total of 1258 data points sampled from such trajectories were added to the initial data set of 244 points.

Batches of 1000 trajectories for the reactions between the $DCO^+ + H$ and $COD^+ + H$ species were run at several sizes of the interpolation data set in order to determine the convergence of the reaction probability with respect to the size of the data set. Batches of 5000 trajectories were calculated for the final data set of 1502 points in order to deter-

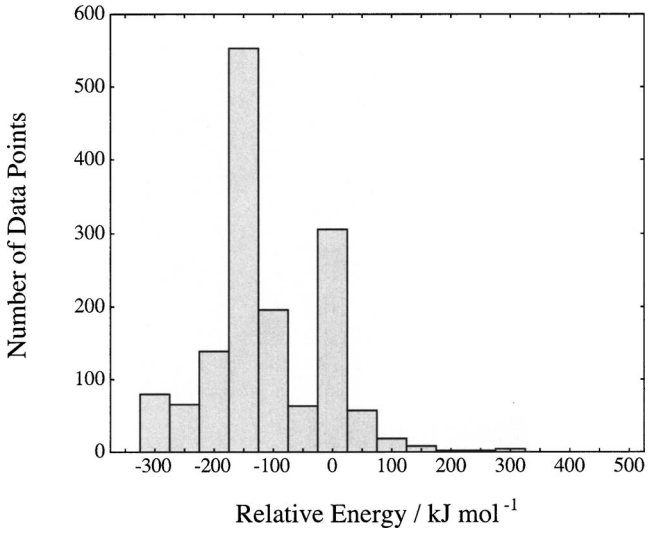

FIG. 2. The distribution of the QCISD/cc-pVTZ energies of the data points used for the interpolated PES is shown as a histogram. The energies are given relative to that of structure 12 in Fig. 1.

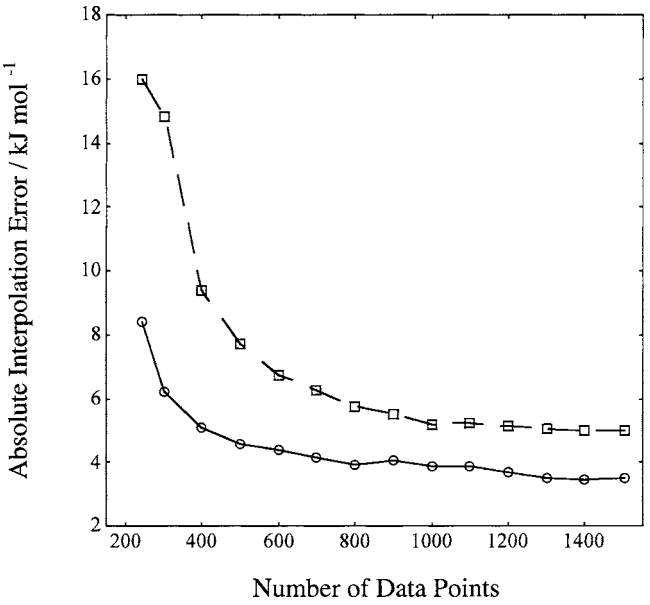

FIG. 3. The convergence of the absolute interpolation error for a sample of 3379 configurations is indicated by the mean (□) and median (○) errors as functions of the size of the data set.

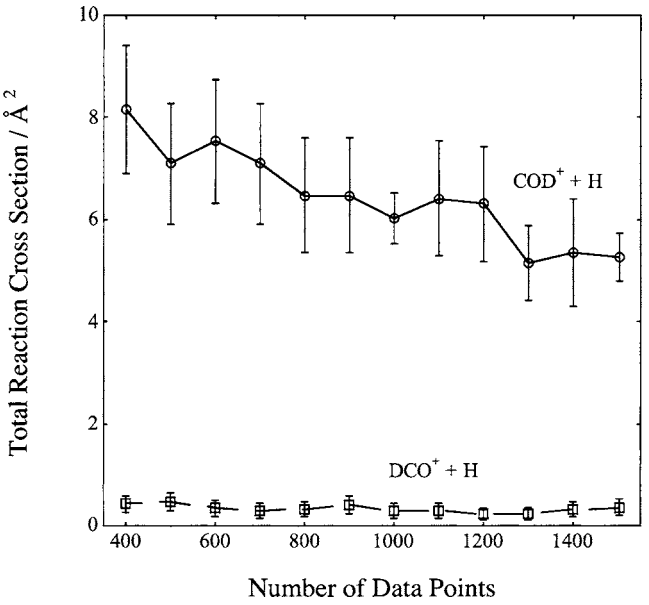

FIG. 4. The total cross sections for all products from COD^++H (○) and DCO^++H (□) are shown as a function of the size of the data set. The error bars indicate two standard deviations associated with the finite trajectory samples.

mine the cross sections for the reactive collisions of (1) COD^++H, (2) COH^++D, (3) COH^++H, (4) DCO^++H, and (5) HCO^++D. The relative kinetic energies given to the fragments were 13.13 kJ mol^{-1} for cases (1)–(3) and 26.25 kJ mol^{-1} for cases (4) and (5). The impact parameters b for the trajectories were sampled randomly from a distribution limited by a maximum exceeding the largest value at which reaction was obtained with the given initial conditions. The distributions of b values were such that the probability of a trajectory having an impact parameter between b and $b+db$ was proportional to b.

III. POTENTIAL ENERGY SURFACE AND DYNAMICS

A. Characteristics of the interpolated PES

The final PES was interpolated over a data set of 1502 points. Figure 2 shows a histogram of the distribution of the energy values for the data set. There are two maxima on the distribution at about −150 and 0 kJ mol^{-1}, which correspond approximately to the energies of the separated fragments COH^++H and HCO^++H. A few very high energy points were sampled during the iterative process, when the accuracy of the PES was low in some regions.

The convergence of the PES was monitored at all stages during the iterative process by calculating the interpolation error (the difference between the *ab initio* and the interpolated energy) for a large number of configurations which were sampled at random from trajectories. The sample contained 3379 points taken from collision trajectories between DCO^+/COD^+ and H, which cover an energy range of 337.3 kJ mol^{-1}. The variation of the median and average interpolation errors for this sample with respect to the number of points in the data set is presented in Fig. 3. With the PES interpolated over a data set size of 1502 points we obtain an average interpolation error of 5.0 kJ mol^{-1} and a median error of 3.5 kJ mol^{-1}. The latter number represents an error of about 1% of the range of energies in the sample. Most importantly, the cross sections for the reactions studied in this paper are reasonably well converged as a function of the size of the data set. This is illustrated in Fig. 4, where the total reaction cross sections for the collisions between COD^++H and DCO^++H are shown as a function of the data set size. Given the statistical errors resulting from the classical simulations, it appears that the total cross section for reaction (3.1) is converged to a value of about 6±1 Å^2, while the cross section for reaction (3.4) is converged to 0.3±0.06 Å^2.

TABLE V. The classical cross sections (Å^2) are shown for reactions (3.1)–(3.5). The errors indicate two standard deviations based on 5000 trajectories for each reaction.

Reactants	Energy (kJ/mol)	Exchange	Isomerization	Isomerization and exchange	Total	Langevin value
$D+COH^+$	13.1	0	0.6±0.2	5.8±0.6	6.4±0.6	24.1
$H+COD^+$	13.1	0	1.0±0.2	4.2±0.4	5.3±0.4	24.1
$H+COH^+$	13.1	0	0.7±0.2	4.6±0.4	5.3±0.6	24.1
$H+DCO^+$	26.3	0.3±0.06	0	0	0.3±0.06	17.1
$D+HCO^+$	26.3	0.7±0.1	0	0	0.7±0.1	17.1

B. Classical dynamics for hydrogen exchange and isomerization

Several product channels were observed during the classical collisions between DCO^+/COD^+ and H/D atoms for the initial conditions reported. They were of three types: isomerization of the isoformyl cation, hydrogen/deuterium exchange occurring during the collisions between formyl and hydrogen, and a combination of the isomerization with exchange during the collisions between isoformyl and hydrogen. The corresponding reaction scheme is as follows:

$$D + COH^+ \rightarrow DCO^+ + H \quad (3.1a)$$

$$\rightarrow HCO^+ + D, \quad (3.1b)$$

$$H + COD^+ \rightarrow DCO^+ + H \quad (3.2a)$$

$$\rightarrow HCO^+ + D, \quad (3.2b)$$

$$H + COH^+ \rightarrow HCO^+ + H, \quad (3.3)$$

$$H + DCO^+ \rightarrow HCO^+ + D, \quad (3.4)$$

$$D + HCO^+ \rightarrow DCO^+ + H. \quad (3.5)$$

Table V reports the classical cross sections for these reactions as calculated from the trajectories, along with the predictions based on the Langevin model for comparison [using the polarizability of the H (or D) atom calculated at the UHF/cc-pVTZ level of theory]. The total reaction cross sections from the classical simulations are very low for all cases (less than 10.0 $Å^2$) and smaller than the Langevin cross sections calculated at the corresponding initial relative translational energies. Previous classical studies on interpolated surfaces, for collisions between ions and neutrals at low translational energies,[20] have also shown that the Langevin values can overestimate the cross sections for reaction. The Langevin cross sections are limited as a reference value for this case, as they neither differentiate between the formyl/isoformyl cations nor account for isotope substitution. Of course, neither the Langevin model nor classical simulations take into account quantum effects, which are very likely to affect the hydrogen/deuterium exchange in these collisions.

Considering the classical cross sections for each reaction channel, we note that the isoformyl cation is the most reactive of the isomers, which is consistent with the quantum chemistry energies and the observations referred to in the previous sections. For the isoformyl cation, the most probable of the reaction channels is a combination of atomic (H/D) exchange with conversion to the formyl form as represented in (3.1a) and (3.2b). Therefore, the outcome of reaction (3.3) is due mainly to isomerization combined with atom exchange, similar to (3.1a) and (3.2b); the classical cross section for this combined process is approximately ten times larger than that of the pure isomerization. Pure atomic exchange in isoformyl without isomerization does not occur in the classical dynamics. The deuterated form of the isoformyl cation is more reactive to pure isomerization than the protonic one, the corresponding classical cross sections being different by nearly a factor of 2. These classical results are seemingly consistent with the hypothesis of a catalytic action of the colliding hydrogen/deuterium in the isomerization of the isoformyl cation. However, the larger cross section for combined isomerization/exchange compared to the pure isomerization suggests a more complex process than the chaperone mechanism. The saddle point for the chaperone mechanism (structure 11) lies at an energy above the total energy of the reactants, so that this mechanism does not contribute to isomerization under the conditions studied here. In contrast to the proton-transport catalysis reported in the literature,[7–9] we see that the atomic exchange which occurs here strongly promotes the isomerization. Hence, H/D atoms can be effective in promoting both isomerization and exchange under the conditions studied here. The absence of barriers in the entrance channel, at the high level of *ab initio* theory employed here, suggests that this reactivity might also be observed under the conditions of the ISM.

The classical cross section for deuteration of the isoformyl ion is larger than that for the release of deuterium atoms from the product (deuterated formyl), which is in agreement with the hypothesis about the key role of reaction (3.1a) in the fractionation of deuterium in the ISM.

Only one reaction channel, exchange, is observed for the collisions of H/D with the formyl cation. For low energy collisions, this exchange of H/D with the formyl cation is not facile. Raising the initial relative kinetic energy to 26.3 kJ mol^{-1} yields total exchange cross sections that are less than 1 $Å^2$. Deuteration of the cation is again preferred over the release of deuterium by collision of deuterated formyl with hydrogen, the corresponding classical cross sections being different by about a factor of 2. This preference for deuteration over the release of deuterium is consistent with the experimental rates reported by Adams and Smith[5] for reaction (3.5) and its reverse (3.4) at temperatures higher than in the ISM. They observed that the isotope fractionation occurred (i.e., the deuteration of the cation) at a rate about 4.5 times faster than the reverse reaction at 300 K, with the ratio of forward/reverse rates becoming greater at lower temperatures.

IV. CONCLUDING REMARKS

An accurate *ab initio* interpolated PES has been constructed to describe the dynamics of the reactions between $HCO^+ + H$, $HOC^+ + H$, and deuterated analogues. This PES is based on a combination of QCISD/cc-pVTZ energies with QCISD/6-311G(d,p) first and second energy derivatives for 1502 molecular configurations. An *ab initio* study of the stationary points on the PES, more accurate than previously reported, has been presented. This study showed that even though the qualitative topography of the PES and the molecular geometries were well described at the HF level, the relative energies of the stationary points are significantly different from the values given by more reliable *ab initio* levels. Although the interpolation error in this PES is only about 1% of the relevant energy range, it is important to pursue further methodology development to accelerate the rate of convergence to high interpolation accuracy.

Classical dynamics on the interpolated PES demonstrate

that isomerization and exchange reactions do occur in collisions of H/D with the isoformyl cation. The calculated cross sections are all very much smaller than the values predicted by the Langevin model at this level of *ab initio* theory. Figure 1 and Table II indicate that there are local maxima and minima in the PES for relatively large separations of the H atom and cation. The minima are not sufficiently deep to trap the incoming atom, nor are the local maxima actual barriers. However, the PES does not support a simple monotonically attractive force in the entrance valley, which may explain the reduced cross sections, relative to the simple Langevin model.

In the conditions of the ISM the overall rate for the isomerization could be strongly determined by quantum effects. In further work, it might be useful to investigate whether the use of quasiclassical, rather than microcanonical, trajectory initial conditions has any significant impact on the data distribution or calculated cross sections. However, the classical dynamics is consistent with experimental measurements and astrochemical models, which suggest that reactions (3.1a) and (3.5) can contribute to the fractionation of deuterium in the ISM.

The software and data for the interpolated PES reported here are available as EPAPS documents.[21] The GROW software is available from the authors upon request.

ACKNOWLEDGMENT

The authors would like to thank the Australian Partnership for Advanced Computing National Facility for an allocation of computer time.

[1] C. Savage and L. M. Ziurys, Astrophys. J. **616**, 966 (2004).
[2] H. Liszt, R. Lucas, and J. H. Black, Astron. Astrophys. **428**, 117 (2004).
[3] S. Green, Astrophys. J. **277**, 900 (1984).
[4] M. Opendak, Astrophys. J. **406**, 548 (1993); T. J. Millar, A. Bennet, and E. Herbst, *ibid.* **340**, 906 (1989).
[5] N. G. Adams and D. Smith, Astrophys. J. **294**, L63 (1985).
[6] Y. Yamaguchi, C. A. Richards, and H. F. Schaefer, J. Chem. Phys. **101**, 8945 (1994).
[7] A. J. Chalk and L. Radom, J. Am. Chem. Soc. **119**, 7573 (1997).
[8] M. A. Collins, S. Petrie, A. J. Chalk, and L. Radom, J. Chem. Phys. **112**, 6625 (2000).
[9] M. A. Collins and L. Radom, J. Chem. Phys. **118**, 6222 (2003).
[10] N. L. Ma, B. J. Smith, J. A. Pople, and L. Radom, J. Am. Chem. Soc. **113**, 7903 (1991).
[11] R. P. A. Bettens and M. A. Collins, J. Chem. Phys. **111**, 816 (1999).
[12] M. A. Collins, Theor. Chem. Acc. **108**, 313 (2002).
[13] M. J. T. Jordan, K. C. Thompson, and M. A. Collins, J. Chem. Phys. **102**, 5647 (1995).
[14] K. C. Thompson and M. A. Collins, J. Chem. Soc., Faraday Trans. **93**, 871 (1997).
[15] J. Ischtwan and M. A. Collins, J. Chem. Phys. **100**, 8080 (1994).
[16] M. J. Frisch, G. W. Trucks, H. B. Schlegel *et al.*, GAUSSIAN 98, Gaussian, Inc., Pittsburgh, PA, 1998.
[17] M. J. Frisch, G. W. Trucks, H. B. Schlegel *et al.*, GAUSSIAN 03, Gaussian, Inc., Pittsburgh, PA, 2004.
[18] N. L. Ma, Ph.D. thesis, Australian National University, 1992.
[19] H. W. Schranz, S. Nordholm, and G. Nyman, J. Chem. Phys. **94**, 1487 (1991).
[20] G. E. Moyano, D. Pearson, and M. A. Collins, J. Chem. Phys. **121**, 12396 (2004).
[21] See EPAPS Document No. E-JCPSA6-124-009612 for the data file and software to evaluate the PES. This document can be reached via a direct link in the online article's HTML reference section or via the EPAPS homepage (http://www.aip.org/pubservs/epaps.html).